

VU Research Portal

Shape corrections to exchange-correlation potentials by gradient-regulated seamless connection of model potentials for inner and outer region

Gruning, M.; Gritsenko, O.V.; van Gisbergen, S.J.A.; Baerends, E.J.

published in

Journal of Chemical Physics
2001

DOI (link to publisher)

[10.1063/1.1327260](https://doi.org/10.1063/1.1327260)

document version

Publisher's PDF, also known as Version of record

[Link to publication in VU Research Portal](#)

citation for published version (APA)

Gruning, M., Gritsenko, O. V., van Gisbergen, S. J. A., & Baerends, E. J. (2001). Shape corrections to exchange-correlation potentials by gradient-regulated seamless connection of model potentials for inner and outer region. *Journal of Chemical Physics*, 114(2), 652-660. <https://doi.org/10.1063/1.1327260>

General rights

Copyright and moral rights for the publications made accessible in the public portal are retained by the authors and/or other copyright owners and it is a condition of accessing publications that users recognise and abide by the legal requirements associated with these rights.

- Users may download and print one copy of any publication from the public portal for the purpose of private study or research.
- You may not further distribute the material or use it for any profit-making activity or commercial gain
- You may freely distribute the URL identifying the publication in the public portal ?

Take down policy

If you believe that this document breaches copyright please contact us providing details, and we will remove access to the work immediately and investigate your claim.

E-mail address:

vuresearchportal.ub@vu.nl

Shape corrections to exchange-correlation potentials by gradient-regulated seamless connection of model potentials for inner and outer region

M. Grüning, O. V. Gritsenko, S. J. A. van Gisbergen, and E. J. Baerends
*Scheikundig Laboratorium der Vrije Universiteit, De Boelelaan 1083, 1081 HV Amsterdam,
 The Netherlands*

(Received 20 July 2000; accepted 28 September 2000)

Shape corrections to the standard approximate Kohn-Sham exchange-correlation (xc) potentials are considered with the aim to improve the excitation energies (especially for higher excitations) calculated with time-dependent density functional perturbation theory. A scheme of gradient-regulated connection (GRAC) of inner to outer parts of a model potential is developed. Asymptotic corrections based either on the potential of Fermi and Amaldi or van Leeuwen and Baerends (LB) are seamlessly connected to the (shifted) xc potential of Becke and Perdew (BP) with the GRAC procedure, and are employed to calculate the vertical excitation energies of the prototype molecules N_2 , CO, CH_2O , C_2H_4 , C_5NH_5 , C_6H_6 , Li_2 , Na_2 , K_2 . The results are compared with those of the alternative interpolation scheme of Tozer and Handy as well as with the results of the potential obtained with the statistical averaging of (model) orbital potentials. Various asymptotically corrected potentials produce high quality excitation energies, which in quite a few cases approach the benchmark accuracy of 0.1 eV for the electronic spectra. Based on these results, the potential BP-GRAC-LB is proposed for molecular response calculations, which is a smooth potential and a genuine ‘‘local’’ density functional with an analytical representation. © 2001 American Institute of Physics. [DOI: 10.1063/1.1327260]

I. INTRODUCTION

The recent success of the time-dependent density functional perturbation theory (TDDFPT)^{1–4} in calculations of electron excitations^{5–12} and other molecular response properties^{13–17} is due to its efficient treatment of electron exchange and correlation. The exchange-correlation (xc) effects in the ground state are represented with the local, state independent exchange-correlation potential v_{xc} in the one-electron Kohn-Sham (KS) equations

$$\left\{ -\frac{1}{2}\nabla^2 + v_{\text{ext}}(\mathbf{r}) + v_H(\mathbf{r}) + v_{xc\sigma}(\mathbf{r}) \right\} \psi_{i\sigma}(\mathbf{r}) = \epsilon_{i\sigma} \psi_{i\sigma}(\mathbf{r}). \quad (1.1)$$

Here v_{ext} is the external potential of the nuclei and v_H is the Hartree potential of electrostatic repulsion which, together with v_{xc} , define the KS orbitals ψ_i and orbital energies ϵ_i . Since the exact form of v_{xc} is not known, various approximations are currently in use. A change of v_{xc} in response to the density change caused by a perturbation $\delta v_{\text{ext}}(\mathbf{r}, \omega)$ of the external potential with the frequency ω is represented with the xc kernel $f_{xc}(\mathbf{r}, \mathbf{r}', \omega)$. Usually, the simple frequency-independent adiabatic local density approximation (ALDA) is employed for f_{xc} ,

$$f_{xc}^{\text{ALDA}}(\mathbf{r}, \mathbf{r}', \omega) = \delta(\mathbf{r} - \mathbf{r}') \left. \frac{dv_{xc}^{\text{LDA}}(\mathbf{r})}{d\rho(\mathbf{r}')} \right|_{\rho=\rho_{\text{SCF}}}, \quad (1.2)$$

where v_{xc}^{LDA} is the xc potential of the local density approximation (LDA). The zero order of TDDFPT for excitation energies is just the difference $\Delta\epsilon_{ia} = \epsilon_a - \epsilon_i$ between the energies of the corresponding occupied ψ_i and unoccupied ψ_a KS orbitals. The correction to $\Delta\epsilon_{ia}$ comes from the coupling

of the single excitations $\varphi_i \rightarrow \varphi_a$ with the coupling matrix $K_{ia\sigma, jb\tau}$, which includes two-electron Coulomb integrals, as well as integrals with the xc kernel f_{xc} .^{2,7}

In spite of the success of TDDFPT, the problem remains to provide a uniform high quality for both lowest and higher-lying excitations with model potentials v_{xc} . Here, the traditional LDA and generalized gradient approximations (GGAs) for v_{xc} have met with limited success. Even though LDA produces reasonable lowest excitation energies,^{6,18} it consistently underestimates the zero-order excitation energy $\Delta\epsilon_{ia}$ for higher excitations. The LDA xc potential v_{xc}^{LDA} is not attractive enough in the molecular bulk region where the occupied and lowest unoccupied orbitals are localized, so that the corresponding orbital energies are too high (not negative enough). In particular, the LDA energy ϵ_N^{LDA} of the highest occupied molecular orbital (HOMO) is much higher (less negative) than the value $\epsilon_N = -I_p$ (I_p is the ionization potential) required by the rigorous KS theory. [Formally, $\epsilon_N = -I_p + v_{xc}(\infty)$, but in order to have consistent comparisons, we will fix the arbitrary uniform constant by which the KS potential may be shifted by requiring the potential to go to zero asymptotically, i.e., $v_{xc}(\infty) = 0$.]

It was an old notion of the $X\alpha$ theory¹⁹ that reasonable ϵ_N values can be obtained with the $X\alpha$ potential with $\alpha = 1.0$, which is 1.5 times as attractive as the LDA exchange potential v_x^{LDA} , the dominant part of v_{xc}^{LDA} : $v_{x\alpha}(\alpha = 1.0) = 1.5v_x^{\text{LDA}}$. The potential $1.5v_x^{\text{LDA}}$ is in fact the electron gas approximation to the exchange hole potential v_x^{hole} that features in the exchange energy, $E_x = (1/2) \int \rho v_x^{\text{hole}} dr$. In the variation procedure to obtain one-electron equations a factor

2/3 is introduced to give $v_{x\alpha}(\alpha=0.667)=v_x^{\text{LDA}}$ as an exchange potential in the one-electron equations. In Refs. 20 and 21, with the partitioning of the exchange potential v_x into the attractive potential of the exchange hole and the repulsive ‘‘response’’ potential, $v_x=v_x^{\text{hole}}+v_x^{\text{resp}}$, the above-mentioned deficiency of v_{xc}^{LDA} has been attributed to a too repulsive character of the LDA response potential $v_x^{\text{resp(LDA)}}$. Indeed, the LDA hole potential is just 1.5 times as attractive as v_x^{LDA} , $v_x^{\text{hole(LDA)}}=1.5v_x^{\text{LDA}}$, and the LDA response potential amounts to minus half of v_x^{LDA} , $v_x^{\text{resp(LDA)}}=-0.5v_x^{\text{LDA}}$, while the true response potential v_x^{resp} should almost vanish in the region of the HOMO.^{20,21} Due to this deficiency, LDA (and GGA) significantly and systematically puts the highest occupied orbitals at too high one-electron energies. The LDA potential, being not deep enough, does not support enough virtual levels, in particular the Rydberg levels with energies close to the energy zero have a much too small gap with respect to the HOMO. The distortion is usually less severe for low-lying virtuals, which are located in roughly the same region of space as the HOMO. So LDA and GGA underestimate vertical excitation energies for the higher-lying excitations, i.e., to one-electron levels which approach the energy zero. It therefore overestimates (hyper)polarizabilities and their frequency dependence for molecules that have relatively large HOMO-LUMO (lowest unoccupied molecular orbital) gaps and thus low polarizabilities arising from high-lying excitations.^{3,4,6,11,22} Standard density gradient GGA corrections to v_{xc}^{LDA} do not produce a substantial improvement of the results.

Thus, accurate modeling of v_{xc} becomes an actual problem of TDDFPT. It should be noted that not only a correction is required in the far asymptotic region, to the effect that the exponential decay of the LDA potential in the outer density tail has to be replaced by a $-1/r$ behavior, but a more general shape correction is needed to adjust in particular the spacing between the occupied orbitals and the high-lying virtuals (low virtuals seem to be quite reasonable in LDA and GGA potentials). In principle, an improved model can be developed either by correction of the standard LDA or GGA potentials, or one can consider an entirely different model of the response potential and, in general, of v_{xc} . The latter option has been followed in the construction of the LB potential in Ref. 23, which both corrects the HOMO energy to close to $-I_p$ and introduces a proper $-1/r$ behavior asymptotically. The LB potential has deficiencies in the inner molecular regions, and in our previous publications^{12,24,25} an orbital-dependent model xc potential v_{xc}^{SAOP} has been constructed by statistical averaging of (model) orbital potentials (SAOP). Within the averaging, for core and deep valence orbitals the GLLB potential $v_{xc}^{\text{GLLB21,26}}$ is used with a response part that correctly reproduces the atomic shell structure in the inner regions, while in the outer valence region the modified LB potential $v_{xc}^{\text{LB}\alpha 23}$ is employed, which reproduces the correct long-range asymptotics of v_{xc} ,

$$v_{xc}(\mathbf{r}) \rightarrow -\frac{1}{r} + v_{xc}(\infty), \quad (1.3)$$

with $v_{xc}(\infty)=0$. The statistical averaging makes the resulting

potential v_{xc}^{SAOP} close to v_{xc}^{GLLB} in the inner region and close to $v_{xc}^{\text{LB}\alpha}$ in the outer region, thus providing a balanced approximation to v_{xc} in all regions. The purpose of SAOP was to provide an improvement not only for the higher-lying, but also for the lowest calculated excitations. SAOP yields a good quality of all calculated excitation energies and other response properties for some small prototype molecules.¹²

In Refs. 27 and 9 the standard LDA and GGA xc potentials, respectively, have been corrected. In Ref. 27 the LDA potential v_{xc}^{LDA} has been shifted in the bulk region downward by $(I_p + \epsilon_N^{\text{LDA}})$, where I_p and ϵ_N^{LDA} have been precalculated with additional self-consistent field (ΔSCF) calculations of the neutral molecule and its cation. In the asymptotic region ($\sim 4\text{-}5$ a.u. from the nearest nucleus) v_{xc}^{LDA} has been replaced with the LB potential v_{xc}^{LB23} with the correct Coulombic behavior (1.3) and zero asymptotics $v_{xc}(\infty)=0$. The total asymptotically corrected potential $v_{xc}^{\text{LDA-AC}}$ is defined simply as the maximum of those two potentials $v_{xc}^{\text{LDA-AC}}(r) = \max[v_{xc}^{\text{LDA}}(r) - (I_p + \epsilon_N), v_{xc}^{\text{LB}}(r)]$. The disadvantage of this simple correction is that, by construction, the potential $v_{xc}^{\text{LDA-AC}}$ possesses a discontinuity in its derivative.

In Ref. 9 the unmodified GGA Hamprecht-Cohen-Tozer-Handy (HCTH) potential v_{xc}^{HCTH} has been used in the bulk region, while the asymptotics (1.3) has been provided with the Fermi-Amaldi potential $v^{\text{FA}}(\mathbf{r}) = -v_H(\mathbf{r})/N$, which is shifted upward by $(I_p + \epsilon_N)$. Thus, the resulting asymptotically corrected potential $v_{xc}^{\text{HCTH-AC}}$ asymptotically goes to a positive constant, $v_{xc}^{\text{HCTH-AC}}(\infty) = (I_p + \epsilon_N)$. The potential v_{xc}^{HCTH} is retained in the spherical regions around the nuclei $\{A\}$ and the asymptotic correction $[v^{\text{FA}}(\mathbf{r}) = -v_H(\mathbf{r})/N + (I_p + \epsilon_N)]$ is switched on by linear interpolation in the intermediate region. The corresponding interpolation function contains explicit electron-nuclear distances r_A (see the next section for the corresponding formula), so that $v_{xc}^{\text{HCTH-AC}}$ is defined on a grid. Both downward shift of the bulk potential in Ref. 27 and upward shift of the asymptotic potential in Ref. 9 are equivalent in the sense that they have the same effect on the orbital energy difference $\Delta\epsilon_{ia}$, while the absolute shift of the total xc potential is immaterial, since the latter is defined up to an arbitrary constant (see the next section for further discussion). The corrections of Refs. 27 and 9 have produced considerable improvement of the calculated molecular response properties. Still, further improvement of model xc potentials is desirable.

In this paper the connection schemes of Refs. 27 and 9 are improved by introducing a density gradient-regulated connection method (GRAC) between bulk and asymptotic potentials, which is presented in Sec. II. This scheme allows us to construct smooth asymptotically corrected potentials, which are genuine density functionals with an analytical representation. In Sec. III, GRAC together with the GGA bulk potential of Becke²⁸ and Perdew²⁹ (BP), and with the LB and FA asymptotic potentials, is applied to the TDDFPT calculations of the vertical excitation energies of the prototype molecules N_2 , CO , CH_2O , C_2H_4 , C_5NH_5 , C_6H_6 , Li_2 , Na_2 , K_2 . The results are compared with those obtained with the linear interpolation function of Ref. 9 as well as with SAOP. In Sec. IV the conclusions are drawn.

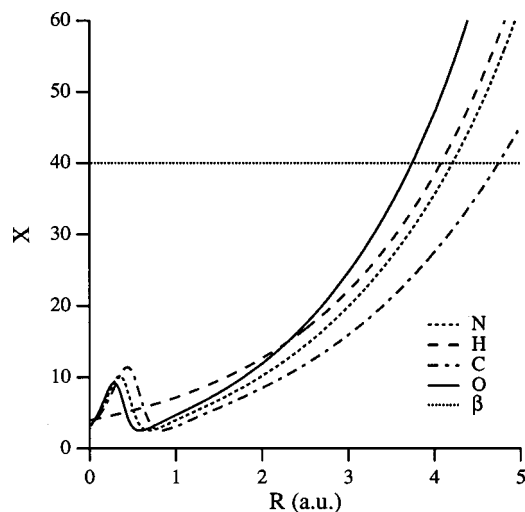


FIG. 1. Form of the density-gradient function $x(\mathbf{r})$ for the H, C, N, O atoms (the straight line indicates the value of the β parameter).

II. GRADIENT-REGULATED CONNECTION BETWEEN BULK AND ASYMPTOTIC POTENTIALS

In general, an asymptotically corrected xc potential v_{xc}^{b-AC} can be written in the following form:

$$v_{xc}^{b-AC}(\mathbf{r}) = [1 - f(\mathbf{r})]v_{xc}^b(\mathbf{r}) + f(\mathbf{r})v_{xc}^a(\mathbf{r}), \quad (2.1)$$

where v_{xc}^b is a potential in the bulk region, which is to be corrected, v_{xc}^a is an asymptotic correction in the region of atomic and molecular density tails, and f is an interpolation or switching function, which is close to 1 in the asymptotic region and vanishes in the bulk region. It is desirable that, with a proper choice of $f(\mathbf{r})$, the corrected potential v_{xc}^{b-AC} be a smooth potential and also a genuine density functional, which has an analytical representation and which possesses usual scaling and invariance properties.

In this paper we propose to use a gradient-regulated asymptotic correction (GRAC), i.e., we employ the standard dimensionless density-gradient argument x ,

$$x(\mathbf{r}) = \frac{|\nabla\rho(\mathbf{r})|}{\rho^{4/3}(\mathbf{r})}, \quad (2.2)$$

as a switching parameter of the interpolation function $f[x(\mathbf{r})]$. The argument x appears to be a natural parameter for this purpose, since in the region of the density tails it diverges, $x(\mathbf{r}) \sim \rho^{-1/3}(\mathbf{r})$, while it remains finite in the bulk region. One can see this from Fig. 1, where $x(r)$ is plotted for the atoms H, C, N, O. For heavier atoms C, N, O, oscillations of $x(r)$ in the bulk region with maxima of about 10 reflect the atomic shell structure. Starting from $r = 1$ a.u., $x(r)$ diverges monotonically.

Having this behavior of $x(\mathbf{r})$ in mind, we choose the following form for the interpolation function $f[x(\mathbf{r})]$ in (2.1),

$$f[x(\mathbf{r})] = \frac{1}{1 + e^{-\alpha[x(\mathbf{r}) - \beta]}}, \quad (2.3)$$

which turns to 1 at the asymptotics $x(\mathbf{r}) \rightarrow \infty$ and, depending on the empirical parameters α and β , can be made vanishing

in the bulk region. The parameter β indicates where to switch ($f(x) = 1/2$ for $x = \beta$), while α determines how fast the switching is (with the condition that their product $\alpha\beta$ should be large enough, so that $\exp(\alpha\beta) \gg 1$). The value $\beta = 40$ has been chosen from atomic calculations, which is well above maximum x values in the bulk atomic regions (see Fig. 1). With this value a switch to the asymptotic potential v_{xc}^a occurs as close to the nucleus as possible, yet without perturbing the energies ϵ_i of the occupied KS orbitals, i.e., the values ϵ_i obtained with v_{xc}^{b-AC} are virtually the same as those obtained with the bulk potential v_{xc}^b . For the parameter α the value $\alpha = 0.5$ has been chosen which, together with $\beta = 40$, guarantees that $f[x(\mathbf{r})]$ vanishes in the bulk region. The use of the dimensionless argument x has the advantage that the dimensionless function $f[x(\mathbf{r})]$ does not change scaling properties of the potentials v_{xc}^a and v_{xc}^b within (2.1). The advantage of the proposed GRAC procedure is that switching to an asymptotically correct potential v_{xc}^a occurs naturally, when the argument x of (2.2) indicates the asymptotic region of the density tails.

The basic option of this paper is the GGA BP potential $v_{xc}^{BP}(\rho(\mathbf{r}), \nabla\rho(\mathbf{r}); \mathbf{r})$ as the bulk potential and the LB potential $v_{xc}^{LB}(\rho(\mathbf{r}), x(\mathbf{r}); \mathbf{r})$ as the asymptotic potential

$$\begin{aligned} v_{xc}^{BP-GRAC}(\rho(\mathbf{r}), \nabla\rho(\mathbf{r}); \mathbf{r}) &= [1 - f[x(\mathbf{r})]]v_{xc}^{BP}(\rho(\mathbf{r}), \nabla\rho(\mathbf{r}); \mathbf{r}) + f[x(\mathbf{r})] \\ &\times [v_{xc}^{LB}(\rho(\mathbf{r}), \nabla\rho(\mathbf{r}); \mathbf{r}) + (I_p + \epsilon_N)]. \end{aligned} \quad (2.4)$$

All components of the asymptotically corrected potential $v_{xc}^{BP-GRAC}$ of (2.4) are explicit functions of the density ρ and its gradient $\nabla\rho$ (including the second derivatives of ρ with respect to \mathbf{r} in v_{xc}^{BP}), so that $v_{xc}^{BP-GRAC}$ is a genuine density functional, which has an analytical representation and it is a smooth potential. In Eq. (2.4) the constant shift $(I_p + \epsilon_N)$ is added to the asymptotic part, as in Ref. 9, so that (2.4) has the asymptotics

$$v_{xc}^{BP-GRAC}(\mathbf{r}) \rightarrow -\frac{1}{r} + (I_p + \epsilon_N), \quad (2.5)$$

where ϵ_N is the HOMO energy of the potential (2.4) and the Coulombic part $-1/r$ is provided by the LB potential v_{xc}^{LB} . With the choice for positive asymptotics, $v_{xc}^{BP-GRAC}$ has virtually the same ϵ_N as the bulk BP potential v_{xc}^{BP} , and the GGA (as well as LDA) ϵ_N value is substantially smaller (in absolute magnitude) than I_p . However, $v_{xc}^{BP-GRAC}(\mathbf{r})$ is, of course, equivalent to the potential $v_{xc}^{BP-GRAC}(\mathbf{r}) - (I_p + \epsilon_N)$ (here the shift is applied to the total potential), since v_{xc} is defined only up to an arbitrary constant. This latter potential has zero asymptotics and its HOMO energy is just $-I_p$, as required by the rigorous KS theory for potentials with zero asymptotics. As an alternative to (2.4) one can apply a shift to the bulk potential, using $v_{xc}^b = v_{xc}^{BP} + \Delta$, where Δ is determined during the SCF cycles. Starting with $\Delta = -(I_p + \epsilon_N^{LDA/GGA})$ the downward shift of the bulk LDA/GGA potential yields an $\epsilon_N^{(1)}$ value of the corrected potential, which will be close to $-I_p$. The shift can be updated on subsequent cycles, with increment $-(I_p + \epsilon_N^{(n)})$ to be applied on cycle $(n+1)$, to fix the HOMO one-electron energy at $-I_p$. To

determine the shift in either the asymptotic or in the bulk potential, the ionization energy I_p should be obtained with additional calculations of a neutral system and its cation with the standard DFT methods. Bearing in mind that calculation of I_p is a separate step, we use in this paper the experimental I_p values as an input.

The explicit use of the ionization energy might create a problem in the case of a weakly bound molecular complex with fragments of different electronegativity. It is clear in this case that, in order to reproduce excitations which are localized within a certain fragment, one should use the ionization energy of this fragment. A possible remedy for this problem could be partitioning of the molecular volume into fragment regions, so that in each region the expression (2.4) will be calculated with the I_p and ϵ_N values of the corresponding fragment. However, we advocate the use of methods like the present one only for systems that are so strongly connected that I_p and ϵ_N are genuinely global quantities of the system.

Besides v_{xc}^{LB} , we also use the Fermi-Amaldi (FA) potential v^{FA} ,

$$v^{FA}(\mathbf{r}_1) = -\frac{v_H(\mathbf{r}_1)}{N} = -\frac{1}{N} \int \frac{\rho(\mathbf{r}_2)}{|\mathbf{r}_1 - \mathbf{r}_2|} d\mathbf{r}_2, \quad (2.6)$$

as the asymptotic potential in (2.4). From a theoretical point of view, the disadvantage of v^{FA} is that, as follows from (2.6), it is effectively produced with an ‘‘exchange-correlation’’ hole function $-\rho(\mathbf{r}_2)/N$, which is delocalized over the entire system, while the real xc hole is more or less localized around the reference electron at \mathbf{r}_1 . Because of this, application of v^{FA} for large molecules should produce underestimation of the exchange-correlation effects in the nearer asymptotic region.

The present paper also compares the performance of the GRAC interpolation function with the linear interpolation approach of Ref. 9 (which has been characterized in the Introduction) for the same potentials v_{xc}^a and v_{xc}^b . In the latter approach the asymptotically corrected potential v_{xc}^{b-AC} lacks uniform analytical representation and it is defined on the grid in the following way: when the distance r_A from a nucleus $\{A\}$ is less than R_1^A , then $v_{xc}^{b-AC} = v_{xc}^b$; when $R_1^A < r_A < R_2^A$ for M nuclei (and $r_B > R_2^B$ for the others nuclei $\{B\}$), then $v_{xc}^{b-AC} = v_{xc}^b + \mu(v_{xc}^a - v_{xc}^b)$ with

$$\mu = \sum_{A=1}^M \frac{r_A - R_2^A}{R_1^A - R_2^A}; \quad (2.7)$$

when the distances from all atoms are larger than R_2 , then $v_{xc}^{b-AC} = v_{xc}^a$. The radii R_1 and R_2 are determined as follows: $R_1 = \gamma R_{SB}$ and $R_2 = \delta R_{SB}$ where R_{SB} is the Slater-Bragg radius of the atom and $\gamma = 3.5$ and $\delta = 4.7$ are the empirical parameters.

Note that, unlike the standard GGA potentials, virtually all the asymptotically corrected potentials (as well as the SAOP potential) are not functional derivatives of known xc energy functionals. The results of molecular response calculations with asymptotically and otherwise corrected potentials, including those to be presented in the next section, demonstrate that for high quality response properties it is of

TABLE I. Vertical excitation energies (eV) of CO. MAE is the mean absolute error, VMAE is the MAE for the V (valence) excitations and RMAE is the MAE for the Rydberg excitations. Ionization potential I_p corresponds to $-\epsilon_N$ for SAOP and BP and to the input experimental value for GRAC/AC.

Excited state and transition	SAOP	BP	BPacFA	BPgracFA	BPgracLB	Exp ^a
³ $\Pi, \sigma \rightarrow \pi^*(V)$	6.28	6.18	6.19	6.20	6.19	6.32
³ $\Sigma^+, \pi \rightarrow \pi^*(V)$	8.64	8.44	8.44	8.46	8.45	8.51
¹ $\Pi, \sigma \rightarrow \pi^*(V)$	8.56	8.36	8.42	8.46	8.45	8.51
³ $\Delta, \pi \rightarrow \pi^*(V)$	9.37	9.18	9.20	9.22	9.21	9.36
³ $\Sigma^-, \pi \rightarrow \pi^*(V)$	10.03	9.86	9.88	9.91	9.90	9.88
¹ $\Sigma^-, \pi \rightarrow \pi^*(V)$	10.03	9.86	9.88	9.91	9.90	9.88
¹ $\Delta, \pi \rightarrow \pi^*(V)$	10.46	10	10.34	10.37	10.35	10.23
³ $\Sigma^+, \sigma \rightarrow 3s$	10.32	8.98	10.14	10.29	10.39	10.40
¹ $\Sigma^+, \sigma \rightarrow 3s$	10.69	9.1	10.51	10.63	10.79	10.78
³ $\Sigma^+, \sigma \rightarrow 3p\sigma$	11.26	9.48	11.14	11.40	11.40	11.30
¹ $\Sigma^+, \sigma \rightarrow 3p\sigma$	11.41	9.49	11.30	11.53	11.59	11.40
¹ $\Pi, \sigma \rightarrow 3p\pi$	11.58	9.49	11.28	11.40	11.64	11.53
³ $\Pi, \sigma \rightarrow 3p\pi$	11.51	9.51	11.23	11.36	11.54	11.55
¹ $\Sigma^+, \sigma \rightarrow 3d\sigma$	12.59	9.93	12.30	12.44	12.67	12.40
MAE	0.09	1.01	0.14	0.10	0.09	
VMAE	0.11	0.12	0.08	0.08	0.08	
RMAE	0.07	1.91	0.21	0.12	0.10	
I_p	13.62	9.15	14.01	14.01	14.01	

^aReference 12.

primary importance that the shape of the potential be accurate, rather than that the condition be met of being a functional derivative of a given density functional for the exchange-correlation energy.

III. EXCITATION ENERGIES WITH ASYMPTOTICALLY CORRECTED POTENTIALS

Calculations of excitation energies are performed using the RESPONSE module of the Amsterdam Density Functional program (ADF). In order to get results close to the basis set limit, increasing numbers of diffuse functions are added to the standard ADF basis V . We have monitored systematically the improvement of results with increasing numbers of diffuse basis functions and we have selected very large basis sets near to the basis set limit. For all the prototype molecules and pyridine we have added for C, O, and N atoms two $3p$, two $3d$, two $4s$ and two $4f$ diffuse functions, and for the H atom one $2p$ function. In case of benzene for the C atom an even tempered basis set is used ($7s6p2d1f$, with the orbital exponent $Z = \alpha\beta^i$, $i = 1, \dots, n$, $\beta = 1.7$ and α is for the most diffuse $1s$, $2p$, $3d$, respectively, 0.7045, 0.3459 and 1.2182). Linear combinations of atomic orbitals have been removed from the basis sets where linear dependency due to adding a large number of diffuse functions was detected. We estimate the error on calculated energies due to the finite basis sets to be always smaller than 0.1 eV and on average of the order of a few hundredths of an eV. Experimental geometries are used for all molecules (see Ref. 12 for the prototype molecules, Ref. 30 for benzene and Ref. 31 for pyridine).

Tables I–VI compare the vertical excitation energies ω_i calculated with the standard exchange-correlation BP potential, BP with various asymptotic corrections, and with the

TABLE II. Vertical excitation energies (eV) of N₂. MAE is the mean absolute error, VSMAE is the MAE for the *V* (valence) excitations and RSMAE is the MAE for the Rydberg excitations. Ionization potential I_p corresponds to $-\epsilon_N$ for SAOP and BP and to the input experimental value for GRAC/AC.

Excited state and transition	SAOP	BP	BPacFA	BPgracFA	BPgracLB	Exp ^a
³ Σ _u ⁺ , π _u → π _g (V)	7.89	7.91	7.92	7.93	7.92	7.75
³ Π _g , σ _g → π _g (V)	7.81	7.73	7.75	7.75	7.75	8.04
³ Δ _u , π _u → π _g (V)	8.82	8.84	8.86	8.86	8.86	8.88
¹ Π _g , σ _g → π _g (V)	9.31	9.21	9.25	9.27	9.26	9.31
³ Σ _u ⁻ , π _u → π _g (V)	9.66	9.68	9.7	9.72	9.71	9.67
¹ Σ _u ⁻ , π _u → π _g (V)	9.66	9.68	9.7	9.72	9.71	9.92
¹ Δ _u , π _u → π _g (V)	10.21	10.22	10.25	10.27	10.26	10.27
³ Π _u , σ _u → π _g (V)	10.88	10.69	10.72	10.73	10.73	11.19
³ Σ _u ⁺ , σ _g → 3sσ _g	11.85	10.06	11.63	11.87	11.92	12.00
¹ Σ _u ⁺ , σ _g → 3sσ _g	12.26	10.19	12.01	12.22	12.32	12.20
¹ Π _u , σ _g → 3pπ _u	12.97	10.76	12.67	12.87	13.02	12.90
¹ Σ _u ⁺ , σ _g → 3pσ _u	12.88	10.46	12.7	13	13.07	12.98
¹ Π _u , π _u → 3sσ _g	13.23	11.43	13.09	12.87	13.36	13.24
¹ Π _u , σ _u → π _g	13.59	11.59	13.42	13.32	13.49	13.63
¹ Σ _u ⁺ , ...	14.03	11.61	14.01	14.19	14.17	14.25
MAE	0.11	1.1	0.20	0.15	0.13	
VSMAE	0.11	0.13	0.12	0.11	0.11	
RSMAE	0.12	1.92	0.27	0.18	0.15	
I_p	15.19	10.36	15.59	15.59	15.59	

^aReference 12.

SAOP potential for small prototype molecules N₂, CO, CH₂O, C₂H₄ and larger aromatic systems C₅NH₅, C₆H₆. The ω_i values have been obtained from the solution of the eigenvalue problem $\Omega F_i = \omega_i^2 F_i$, where

$$\begin{aligned} \Omega_{ia\sigma, jb\tau} = & \delta_{\sigma\tau} \delta_{ij} \delta_{ab} (\epsilon_{a\sigma} - \epsilon_{i\sigma})^2 \\ & + 2\sqrt{(\epsilon_{a\sigma} - \epsilon_{i\sigma})(\epsilon_{b\sigma} - \epsilon_{j\sigma})} \int d\mathbf{r} \int d\mathbf{r}' \\ & \times \psi_{i\sigma}(\mathbf{r}) \psi_{a\sigma}(\mathbf{r}) \left[\frac{1}{|\mathbf{r} - \mathbf{r}'|} + f_{xc}^{\sigma\rho(\text{ALDA})}(\mathbf{r}, \mathbf{r}') \right] \\ & \times \psi_{j\tau}(\mathbf{r}') \psi_{b\tau}(\mathbf{r}') \end{aligned} \quad (3.1)$$

(real orbitals are considered). The ALDA xc kernel (1.2) has been used in all cases and, as follows from the previous discussion, asymptotic corrections to BP alter only the orbital energy differences in (3.1) and, to some extent, the form of the unoccupied KS orbitals $\psi_{a\sigma}(\mathbf{r})$. The asymptotically corrected potentials to be compared are BP-GRAC-LB of Eq. (2.4), BP-GRAC-FA with the gradient-dependent switching function (2.3) and the FA asymptotic potential (2.6) as well as the analogous potential BP-AC-FA with the linear interpolation function (2.7).

The TDDFPT excitation energies are compared with reference data. For N₂, CO, CH₂O, C₂H₄ the same experimental data are used as in Ref. 12, while for C₅NH₅ and C₆H₆ the energies are taken from experiment and from calculations in Refs. 32 and 33 with the *ab initio* complete active space multiconfigurational self-consistent-field method with addition of second-order perturbation theory corrections (CASPT2). Tables I–VI also present the mean absolute error (MAE) with respect to the reference values for all excitations and separately the mean absolute errors for the excitations to

TABLE III. Vertical excitation energies (eV) of CH₂O. MAE is the mean absolute error, VSMAE is the MAE for the *V* (valence) excitations and RSMAE is the MAE for the Rydberg excitations. Ionization potential I_p corresponds to $-\epsilon_N$ for SAOP and BP and to the input experimental value for GRAC/AC.

Excited state and transition	SAOP	BP	BPacFA	BPgracFA	BPgracLB	Exp ^a
³ A ₂ , n → π*(V)	3.64	3.31	3.31	3.32	3.31	3.50
¹ A ₂ , n → π*(V)	4.24	3.91	3.92	3.93	3.92	4.10
³ A ₁ , π → π*(V)	6.33	6.24	6.25	6.26	6.25	6.00
³ B ₂ , n → 3s	6.92	5.87	6.7	6.83	6.62	7.09
¹ B ₂ , n → 3s	7.14	5.92	6.87	7.00	6.81	7.13
³ B ₂ , n → 3p _{a1}	8.08	6.49	7.66	7.76	7.72	7.92
¹ B ₂ , n → 3p _{a1}	8.21	6.50	7.79	7.90	7.84	7.98
³ A ₁ , n → 3p _{b2}	8.15	6.51	7.86	7.95	7.80	8.11
¹ A ₁ , n → 3p _{b2}	8.26	6.50	7.96	8.05	7.94	8.14
¹ B ₁ , σ → π*(V)	9.01	8.91	8.92	8.93	8.92	9.00
MAE	0.14	0.93	0.22	0.16	0.23	
VSMAE	0.16	0.18	0.18	0.17	0.18	
RSMAE	0.12	1.43	0.26	0.15	0.27	
I_p	11.02	6.35	10.88	10.88	10.88	

^aReference 12.

valence states (VSMAE) and to Rydberg-like states (RSMAE). In Tables V and VI we mark with (d) states having contributions from double and higher excitations of more than 8% in the configuration interaction wave functions as reported in Ref. 34 and that are insufficiently described within the adiabatic approximation. In this case also the mean absolute error excluding states marked with a (d) is reported in parentheses beside the MAE value.

The results obtained with the uncorrected BP potential are typical for the standard LDA and GGA methods. BP yields a good estimate of the ω_i excitation energies lower than the ionization energy estimated by BP HOMO- ϵ_N . This is reflected in low VSMAE values of BP, 0.1–0.3 eV for all molecules. For Rydberg excitation energies, BP fails to re-

TABLE IV. Vertical excitation energies (eV, from π-orbital) of C₂H₄. MAE is the mean absolute error, VSMAE is the MAE for the *V* (valence) excitations and RSMAE is the MAE for the Rydberg excitations. Ionization potential I_p corresponds to $-\epsilon_N$ for SAOP and BP and to the input experimental value for GRAC/AC.

Excited state and orbital	SAOP	BP	BPacFA	BPgracFA	BPgracLB	Exp ^a
³ B _{1u} , π*(V)	4.64	4.68	4.69	4.69	4.68	4.36
³ B _{3u} , 3s	7.18	6.51	7.10	7.13	7.01	6.98
¹ B _{3u} , 3s	7.29	6.53	7.19	7.22	7.12	7.15
¹ B _{1u} , π*(V)	7.62	7.43	7.62	7.65	7.60	7.66
³ B _{1g} , 3p _y	7.91	7.09	7.81	7.84	7.72	7.79
³ B _{2g} , 3p _z	7.81	6.93	7.77	7.84	7.61	7.79
¹ B _{1g} , 3p _y	8.00	7.10	7.88	7.91	7.84	7.83
¹ B _{2g} , 3p _z	7.94	6.95	7.85	7.92	7.70	8.00
³ A _g , 3p _x	8.70	7.36	8.22	8.26	8.42	8.15
¹ A _g , 3p _x	8.91	7.36	8.36	8.40	8.61	8.29
³ B _{3u} , 3d _{z²}	8.96	7.61	8.70	8.73	8.76	8.57
¹ B _{3u} , 3d _{z²}	9.03	7.64	8.74	8.77	8.79	8.62
MAE	0.25	0.72	0.10	0.11	0.16	
VSMAE	0.16	0.28	0.19	0.17	0.19	
RSMAE	0.28	0.81	0.08	0.10	0.16	
I_p	10.92	6.81	10.52	10.52	10.52	

^aReference 12.

TABLE V. Singlet vertical excitation energies (eV) of C_5NH_5 . MAE is the mean absolute error, VSMAE is the MAE for the V (valence) excitations and R SMAE is the MAE for the Rydberg excitations. Excited states marked with (d) had more than 8% double excitation character, see text. MAE values between parentheses are obtained excluding these states. Ionization potential I_p corresponds to $-\epsilon_N$ for SAOP and BP and to the input experimental value for GRAC/AC.

Excited state and transition	SAOP	BP	BPacFA	BPgracFA	BPgracLB	Exp/ CASPT2 ^a
$B_2, \pi \rightarrow \pi^*(V)$	5.36	5.38	5.35	5.40	5.38	4.99(d)
$A_1, \pi \rightarrow \pi^*(V)$	6.23	6.24	6.25	6.26	6.23	6.38
$A_1, \pi \rightarrow \pi^*(V)$	7.21	7.19	7.22	7.24	7.12	7.22
$B_2, \pi \rightarrow \pi^*(V)$	7.17	7.09	7.14	7.16	7.08	7.22
$B_1, n \rightarrow \pi^*(V)$	4.55	4.39	4.39	4.39	4.38	4.59(d)
$A_2, n \rightarrow \pi^*(V)$	4.72	4.49	4.50	4.50	4.49	5.43(d)
$A_1, \pi(a_1) \rightarrow 3s$	6.38	5.46	6.18	6.28	5.8	6.28
$A_2, \pi(a_2) \rightarrow 3s$	6.86	6.53	6.89	6.98	6.51	6.75*
$B_2, \pi(a_1) \rightarrow 3p_x$	7.05	5.86	6.83	6.92	6.4	7.21*
$B_1, \pi(a_2) \rightarrow 3p_x$	7.57	6.59	7.52	7.57	7.13	7.25*
$B_1, n \rightarrow 3s$	7.53	6.8	8.33	7.61	7.14	7.39*
$A_1, \pi(a_1) \rightarrow 3p_y$	7.3	5.95	7.01	7.09	6.61	7.35*
$A_2, \pi(a_2) \rightarrow 3p_y$	7.79	7.09	7.74	7.82	7.34	7.52*
$A_2, \pi(a_2) \rightarrow 3d_{z^2}$	8.22	7.09	8.08	8.13	7.9	7.98*
$B_2, \pi(a_2) \rightarrow 3p_z$	8.36	6.68	7.55	8	7.87	7.41*
$A_2, n \rightarrow 3p_x$	8.36		8.15	8.4	7.9	8.03*
$B_1, \pi(a_1) \rightarrow 3p_z$	7.82	5.98	7.18	7.23	7.09	7.45*
$B_1, \pi(a_2) \rightarrow 3d_{xy}$	8.24	7.09	8.19	8.28	7.75	8.03*
MAE	0.25 (0.23)	0.67 (0.70)	0.27 (0.23)	0.27 (0.23)	0.34 (0.30)	
VSMAE (V)	0.22	0.31	0.28	0.29	0.32	
R SMAE	0.27	0.86	0.27	0.27	0.34	
I_p	10.24	5.95	9.34	9.34	9.34	

^aReferences 32 and 33.

produce both their absolute values and their relative order. BP consistently and substantially underestimates higher excitations, which leads to large R SMAE values of order of 1 eV for CH_2O , C_2H_4 , C_5NH_5 and of 2 eV for CO and N_2 . Note the lower (though still appreciable) R SMAE of 0.59 eV for the benzene. As a result, the total MAEs of BP are also large.

The corrections to BP considerably improve its performance. By construction, these corrections have relatively little effect on the lower excitations. Due to this, VSMAE values of all corrected potentials are close to the corresponding BP values. Still, in all those cases where corrections alter VSMAE, they always produce an improvement, which is most appreciable for ethylene (see Table IV). But, most importantly, the corrections dramatically improve the calculated higher excitations. In particular, for ethylene and benzene, R SMAE values of all corrected potentials appear to become even smaller than the corresponding VSMAE values. As a result, in all cases the total MAE of the corrected potentials is much smaller than that of the standard BP, and in quite a few cases MAE approaches the benchmark accuracy of 0.1 eV for the electronic spectra.

One can further analyze the performance of various types of asymptotic correction by comparing the results of the corresponding corrected potentials. In particular, the comparison of the results of BP-GRAC-FA and BP-AC-FA allows us to assess the performance of the proposed GRAC function (2.3), since these two potentials differ only in the interpolation functions. On average, BP-GRAC-FA yields somewhat better higher excitations compared to BP-AC-FA.

In particular, for N_2, CO, CH_2O BP-GRAC-FA produces higher energy values and, as a result, its R SMAEs are 0.08–0.12 eV lower than those of BP-AC-FA. We attribute this difference to the fact that the Fermi-distribution-type GRAC function (2.3) switches faster than the linear interpolation function (2.7) to the asymptotic potential, thus effectively producing a less attractive potential in the transition region. It seems also that the GRAC switching is more flexible, since it occurs naturally when the gradient parameter $x(\mathbf{r})$ indicates the density tail region. Thus, for N_2 , for example, the switching (in the direction along the N-N axis) occurs at a distance of less than 4 a.u. from the N atom, whereas for the N atom it occurs at 4.3 a.u. Unlike this, the switching of Ref. 9 in BP-AC-FA is rigidly fixed with the atomic parameters, and it begins at 4.3 a.u. in both cases. Since, as was mentioned before, asymptotic potentials have little influence on the lower excitations, VSMAEs and MAEs of the potentials BP-GRAC-FA and BP-AC-FA are closer to each other than R SMAE, so that the interpolation functions (2.3) and (2.7) exhibit equally good overall performance. This means that in practical calculations one can use the explicit function of the density gradient (2.3).

To assess the effect of the LB asymptotic correction to BP, one can compare the performance of BP-GRAC-LB with BP-GRAC-FA. Besides the common bulk BP part, these two potentials also have the same switching GRAC function, so that the differences in the results will indicate the difference between the asymptotic LB and FA potentials. On average, both potentials produce results of similar good quality with a

TABLE VI. Vertical excitation energies (eV) of C_6H_6 . MAE is the mean absolute error, VSMAE is the MAE for the V (valence) excitations and RSMAE is the MAE for the Rydberg excitations. Excited states marked with (*d*) had more than 8% double excitation character, see text. MAE values between parentheses are obtained excluding these states. Ionization potential I_p corresponds to $-\epsilon_N$ for SAOP and BP and to the input experimental value for GRAC/AC.

Excited state and transition	SAOP	BP	BPacFA	BPgracFA	BPgracLB	Exp/ CASPT2 ^a
$^1B_{2u}, \pi \rightarrow \pi^*(V)$	5.29	5.29	5.32	5.33	5.31	4.90(d)
$^1B_{1u}(V)$	6.06	6.05	6.09	6.09	6.06	6.20
$^1E_{1u}(V)$	6.94	6.55	6.89	6.92	6.86	6.94
$^1E_{2g}(V)$	8.3	8.31	8.40	8.4	8.38	7.90*(d)
$^1E_{1g}, \pi \rightarrow 3s$	6.55	5.96	6.50	6.55	6.22	6.33
$^1A_{2u}, \pi \rightarrow 3p_x, 3p_y$	7.34	6.31	7.12	7.26	6.86	6.93
$^1E_{2u}$	7.33	6.32	7.11	7.25	6.85	6.95
$^1A_{1u}$	7.34	6.35	7.13	7.28	6.85	6.99*
$^1E_{1u}, \pi \rightarrow 3p \pi$	8.1	6.93	7.29	7.29	7.28	7.41
$^1B_{1g}, \pi \rightarrow 3d_{x^2-y^2}, 3d_{xy}$	7.98	6.79	7.70	8.05	7.61	7.46
$^1B_{2g}$	8.03	6.8	7.72	8.09	7.64	7.46
$^1E_{1g}$	8.01	6.8	7.70	8.08	7.63	7.54
$^1A_{1g}, \pi \rightarrow 3d_{xz}, 3d_{zy}$	9.01	7.12	7.95	7.95	8.17	7.74
$^1E_{2g}$	8.91	7.1	7.91	7.91	8.04	7.81
$^1A_{2g}$	8.94	7.14	7.95	7.95	8.1	7.81
$^1E_{1g}, \pi \rightarrow 3d_{z^2}$	7.97	7.05	7.59	7.78	7.49	7.57*
$^3B_{2u}, \pi \rightarrow \pi^*(V)$	5.02	5.02	5.06	5.06	5.04	5.60
$^3B_{1u}(V)$	4.42	4.43	4.47	4.47	4.46	3.94
$^3E_{1u}(V)$	4.77	4.77	4.81	4.81	4.8	4.76
$^3E_{2g}(V)$	7.44	7.45	7.51	7.51	7.49	7.12*
$^3E_{1g}, \pi \rightarrow 3s$	6.51	5.95	6.45	6.53	6.19	6.34*
$^3A_{2u}, \pi \rightarrow 3p_x, 3p_y$	7.28	6.3	7.10	7.24	6.83	6.80*
$^3E_{2u}$	7.31	6.32	7.12	7.26	6.85	6.90*
$^3A_{1u}$	7.34	6.33	7.13	7.28	6.88	7.00*
$^3E_{1u}, \pi \rightarrow 3p \pi$	8.02	6.59	7.22	7.21	7.16	6.98*
$^3B_{1g}, \pi \rightarrow 3d_{x^2-y^2}, 3d_{xy}$	7.98	6.8	7.71	8.06	7.62	7.53*
$^3B_{2g}$	7.93	6.8	7.70	8.05	7.6	7.53*
$^3E_{1g}$	7.95	6.8	7.70	8.05	7.61	7.57*
$^3E_{2g}, \pi \rightarrow 3d_{xz}, 3d_{zy}$	8.29	7.12	7.93	7.93	8.06	7.55*
$^3A_{1g}$	8.85	7.12	7.91	7.91	8.01	7.62*
$^3A_{2g}$	8.94	7.14	7.95	7.95	8.1	7.70*
$^3E_{1g}, \pi \rightarrow 3d_{z^2}$	7.87	7.03	7.54	7.69	7.41	7.56*
MAE	0.53 (0.54)	0.53 (0.54)	0.21 (0.20)	0.32 (0.31)	0.21 (0.19)	
VSMAE	0.29	0.34	0.32	0.32	0.33	
RSMAE	0.61	0.59	0.18	0.32	0.17	
I_p	10.32	6.26	9.25	9.25	9.25	

^aReferences 32 and 33.

slightly better performance of FA for formaldehyde and of LB for benzene.

One can also assess the performance of the bulk BP potential from the comparison of the results of BP-AC-FA with those obtained in Ref. 9 with the asymptotically corrected potential HCTH-AC-FA, where HCTH is the GGA potential, the functional derivative of the HCTH energy functional of Ref. 35. Thus, the present BP-AC-FA and HCTH-AC-FA of Ref. 9 differ only in the bulk part. Both BP-AC-FA and HCTH-AC-FA produce virtually identical MAEs for formaldehyde and ethylene, but for benzene the MAE of 0.14 eV of HCTH-AC-FA is somewhat lower than the 0.21 eV of BP-AC-FA, while for CO and N_2 MAEs of 0.14 and 0.20 eV, respectively, of BP-AC-FA are lower than the corresponding values 0.32 and 0.34 eV of HCTH-AC-FA. From this we can conclude that BP can be recommended for molecular response calculations.

From Tables I–VI one can see also a good performance of the SAOP potential. The quality of its results is similar to

that of the asymptotically corrected potentials and SAOP produces the least MAEs for N_2, CO, CH_2O, C_5NH_5 . Unlike the schemes of asymptotic correction, SAOP employs neither standard GGA bulk potentials, nor the precalculated ionization energies I_p . Instead, the potential v_{xc}^{SAOP} with the zero asymptotics $v_{xc}^{SAOP}(\infty) = 0$ is constructed with statistical averaging of model orbital potentials.^{12,24,25} This potential yields HOMO energies ϵ_N^{SAOP} , which are much closer to the experimental energies $-I_p$ than the ϵ_N^{GGA} values of standard GGAs (See Tables I–VI). The largest deviation between ϵ_N^{SAOP} and $-I_p$ occurs for benzene, with the former quantity being appreciably larger (in absolute magnitude) than the latter (see Table VI). As a result, SAOP consistently overestimates the energies of the higher excitations, which are not far from I_p , and produces in this particular case the largest MAE, VSMAE and RMAE.

Table VII compares the lowest dipole excitation energies calculated for the alkali dimers Li_2, Na_2, K_2 with experimen-

TABLE VII. Lowest dipole-allowed excitation energies and average static polarizabilities α_{av} for alkali dimers. MAE is the mean absolute error of all the excitation energies in this table, MAE(LL) is the mean absolute error for the all low-lying (LL) excitation energies and MAE(HL) for the high-lying.

	Exp ^a	SAOP	BP	BPacFA	BPgracFA	BPgracLB
Li ₂						
¹ Σ _u ⁺ (LL)	1.74	1.98	1.99	1.99	1.98	1.96
¹ Π _u (LL)	2.53	2.46	2.62	2.59	2.55	2.55
¹ Σ _u ⁺	3.78	3.71	3.06	3.63	3.62	3.33
α_{av}	221 ³⁷	223.90	196.90	200.00	204.40	205.06
Na ₂						
¹ Σ _u ⁺ (LL)	1.82	1.96	2.06	2.06	2.04	2.02
¹ Π _u (LL)	2.52	2.51	2.63	2.64	2.59	2.59
¹ Σ _u ⁺	3.64	3.64	3.23	3.49	3.52	3.60
α_{av}	270 ³⁷	233.50	238.00	238.00	243.00	246.00
K ₂						
¹ Σ _u ⁺ (LL)	1.45	1.57	1.54	1.54	1.53	1.50
¹ Π _u (LL)	1.91	2.02	2.00	1.99	1.94	1.92
¹ Σ _u ⁺	2.85	2.62	2.57	2.69	2.69	2.62
¹ Π _u	2.85	2.82	2.70	2.85	2.82	2.78
α_{av}	462.6 (<i>ab initio</i>) ^b	436.10	451.30	451.35	463.32	474.42
MAE		0.10	0.24	0.13	0.11	0.14
MAE(LL)		0.12	0.22	0.21	0.17	0.14
MAE(HL)		0.08	0.39	0.12	0.12	0.20

^aReference 36.

^bReference 38.

tal reference data (Ref. 36 for excitation energies and Ref. 37 for average static polarizability of Li₂ and Na₂, for K₂ *ab initio* value³⁸). The results show the same general trend as for the molecules discussed above. BP reproduces well the lowest excitations to ¹Σ_u⁺ and ¹Π_u states with a somewhat larger error for the ¹Σ_u⁺ state of Na₂. On the other hand, BP consistently underestimates higher ²Σ_u⁺ and ²Π_u excitations. Again, the asymptotic corrections to BP improve the calculated higher excitations, bringing MAE for the dimers close to the benchmark accuracy of 0.1 eV (see Table VII). Note the high quality of the excitation energies obtained with SAOP, which is, on average, even slightly better than those of the asymptotically corrected potentials. Note also a slight improvement of the dipole polarizabilities α_d calculated by the potentials BP-GRAC-FA and BP-GRAC-LB with the GRAC interpolation function, while BP-AC-FA with the linear interpolation function (2.7) produces virtually the same α_d values as BP.

To sum up, the asymptotic corrections to the BP potential provide high overall quality of the calculated excitation energies and a substantial improvement upon the standard BP potential. The corrections dramatically improve the calculated Rydberg-like excitations, while keeping and, sometimes, improving valence excitations. All asymptotic corrections considered display a similar quality of the results, in particular, the present GRAC interpolation function (2.3) performs well with both the FA and LB as the asymptotic potentials.

IV. CONCLUSIONS

In this paper corrections to the standard DFT exchange-correlation potentials have been considered with the aim to improve the excitation energies (especially for higher excitations) calculated within TDDFT. A scheme of gradient-

regulated connection between inner and outer parts (GRAC) has been developed. According to this scheme, the interpolation between the bulk and asymptotic potentials is carried out with an interpolation function, which depends on the dimensionless gradient parameter $x(\mathbf{r})$ of (2.2). Together with a standard GGA potential (as the bulk potential) and with the shifted LB potential (as the asymptotic potential) this interpolation function would constitute a smooth potential $v_{xc}^{GGA-GRAC}(\mathbf{r})$ with an analytical representation. $v_{xc}^{GGA-GRAC}(\mathbf{r})$ would be an explicit ‘‘local’’ density functional in the sense that it depends on quantities, such as the electron density $\rho(\mathbf{r})$ and its gradient $\nabla\rho$, which are evaluated at the point \mathbf{r} .

The corrections to the GGA BP xc potential produced with the GRAC interpolation function, the linear interpolation function of Ref. 9, and with the LB and FA asymptotic potentials have been employed to calculate the vertical excitation energies of the prototype molecules N₂, CO, CH₂O, C₂H₄, C₅NH₅, C₆H₆ as well as the lowest excitation energies of the alkali dimers Li₂, Na₂, K₂. Various asymptotic corrections provide a similar high quality of the calculated excitation energies and a substantial improvement upon the standard BP potential. In quite a few cases the corresponding mean absolute errors of the asymptotically corrected potentials approach the benchmark accuracy of 0.1 eV for the electronic spectra. In particular, the shape corrections substantially improve the calculated Rydberg-like excitations, while retaining and, in some cases, improving the quality of the calculated valence excitations. These results allow us to propose for molecule response calculations the combination BP-GRAC-LB, a smooth potential and a genuine local density functional. Its use does not entail any additional computational effort once a GGA ‘‘bulk’’ potential is evaluated. Our results also confirm the conclusion that for a

variety of small and medium-size molecules high quality TDDFT results can be achieved with the efficient combination of a properly constructed xc potential with the simple ALDA approximation (1.2) for the xc kernel. We stress that asymptotic correction of KS potential is not enough. For instance, the recently developed molecular exact exchange potentials^{39,40} are asymptotically correct but still are not competitive for excitation energy calculations due to general shape deficiencies (lack of the correlation potential contribution).

The schemes of correction of the standard LDA/GGA potentials considered in this paper and in Refs. 9, 27 and the scheme of SAOP offer two alternative ways of improving approximate Kohn-Sham xc potentials. SAOP represents orbital-dependent functionals, it depends on the densities of individual KS orbitals, and the SAOP approach employs essentially differences in spatial localization of these orbitals. As has been shown in this paper, SAOP produces high quality results, though from the point of view of implementation and computation orbital-dependent functionals are more demanding than standard ‘‘local’’ DFT functionals. In this sense, the present scheme of asymptotic correction of LDA/GGA potentials offers an alternative. It uses standard DFT potentials and schemes, such as BP-GRAC-LB developed in this paper, and produces local density functionals. BP-GRAC-LB shares with the asymptotically corrected potentials of Refs. 9 and 27 the disadvantage that it requires as input the ionization energy of the system, which first has to be evaluated in a separate calculation.

¹E. K. U. Gross, J. F. Dobson, and M. Petersilka, in *Density Functional Theory*, edited by R. F. Nalewajski (Springer, Berlin, 1996), Vol. 181, p. 81.

²M. Casida, in *Recent Advances in Density Functional Methods*, edited by D. P. Chong (World Scientific, Singapore, 1995), Vol. 1.

³R. Bauernschmitt and R. Ahlrichs, *Chem. Phys. Lett.* **256**, 454 (1996).

⁴S. J. A. van Gisbergen, J. G. Snijders, and E. J. Baerends, *J. Chem. Phys.* **103**, 9347 (1995).

⁵C. Jamorski, M. Casida, and D. R. Salahub, *J. Chem. Phys.* **104**, 5134 (1996).

⁶M. E. Casida, C. Jamorski, K. C. Casida, and D. R. Salahub, *J. Chem. Phys.* **108**, 4439 (1998).

⁷M. Petersilka, U. J. Gossmann, and E. K. U. Gross, *Phys. Rev. Lett.* **76**, 1212 (1996).

⁸R. Bauernschmitt, M. Haeser, O. Treutler, and R. Ahlrichs, *Chem. Phys. Lett.* **264**, 573 (1997).

⁹D. J. Tozer and N. C. Handy, *J. Chem. Phys.* **109**, 10180 (1998).

¹⁰R. E. Stratman, G. E. Scuseria, and M. J. Frisch, *J. Chem. Phys.* **109**, 8218 (1998).

¹¹S. J. A. van Gisbergen, F. Kootstra, P. R. T. Schipper, O. V. Gritsenko, J. G. Snijders, and E. J. Baerends, *Phys. Rev. A* **57**, 2556 (1998).

¹²P. R. T. Schipper, O. V. Gritsenko, S. J. A. van Gisbergen, and E. J. Baerends, *J. Chem. Phys.* **112**, 1344 (2000).

¹³S. J. A. van Gisbergen, V. P. Osinga, O. V. Gritsenko, R. van Leeuwen, J. G. Snijders, and E. J. Baerends, *J. Chem. Phys.* **105**, 3142 (1996).

¹⁴V. P. Osinga, S. J. A. van Gisbergen, J. G. Snijders, and E. J. Baerends, *J. Chem. Phys.* **106**, 5091 (1997).

¹⁵U. Hohm, D. Goebel, and S. Grimme, *Chem. Phys. Lett.* **272**, 1059 (1997).

¹⁶A. Görling, H. H. Heinze, S. P. Ruzankin, M. Stauffer, and N. Rösch, *J. Chem. Phys.* **110**, 2785 (1999).

¹⁷A. G. Ioannou, S. M. Colwell, and R. D. Amos, *Chem. Phys. Lett.* **278**, 278 (1997).

¹⁸I. Vasiliev, S. Ögüt, and J. R. Chelikowsky, *Phys. Rev. Lett.* **82**, 1919 (1999).

¹⁹J. C. Slater, *Quantum Theory of Molecules and Solids* (McGraw-Hill, New York, 1974), Vol. 4.

²⁰O. V. Gritsenko, R. van Leeuwen, and E. J. Baerends, *J. Chem. Phys.* **101**, 8955 (1994).

²¹O. V. Gritsenko, R. van Leeuwen, E. van Lenthe, and E. J. Baerends, *Phys. Rev. A* **51**, 1944 (1995).

²²S. A. C. McDowell, R. D. Amos, and N. C. Handy, *Chem. Phys. Lett.* **235**, 1 (1995).

²³R. van Leeuwen and E. J. Baerends, *Phys. Rev. A* **49**, 2421 (1994).

²⁴O. V. Gritsenko, P. R. T. Schipper, and E. J. Baerends, *Chem. Phys. Lett.* **302**, 199 (1999).

²⁵O. V. Gritsenko, P. R. T. Schipper, and E. J. Baerends, *Int. J. Quantum Chem.* **76**, 407 (2000).

²⁶O. V. Gritsenko, R. van Leeuwen, and E. J. Baerends, *Int. J. Quantum Chem.* **61**, 231 (1997).

²⁷M. E. Casida, K. C. Casida, and D. R. Salahub, *Int. J. Quantum Chem.* **70**, 933 (1998).

²⁸A. Becke, *Phys. Rev. A* **38**, 3098 (1988).

²⁹J. P. Perdew, *Phys. Rev. B* **33**, 8822 (1986); **34**, 7406 (1986).

³⁰N. C. Handy and D. J. Tozer, *J. Comput. Chem.* **20**, 106 (1999).

³¹J. B. Foresman, M. Head-Gordon, J. A. Pople, and M. J. Frisch, *J. Phys. Chem.* **96**, 135 (1992).

³²C. Adamo, G. E. Scuseria, and V. Barone, *J. Chem. Phys.* **111**, 2889 (1999).

³³J. Lorentzon, P. A. Malmquist, M. Fulscher, and B. O. Roos, *Theor. Chim. Acta* **91**, (1995).

³⁴S. Grimme and M. Waletzke, *J. Chem. Phys.* **111**, 5645 (1999).

³⁵F. A. Hamprecht, A. J. Cohen, D. J. Tozer, and N. C. Handy, *J. Chem. Phys.* **109**, 6264 (1998).

³⁶G. Herzberg, *Spectra of Diatomic Molecules* (Krieger, Malabar, 1989).

³⁷B. Antoine, D. Rayane, A. R. Allouche, M. Aubert-Frecon, E. Benichou, F. W. Dalby, P. Dugourd, and J. Broyer, *J. Chem. Phys.* **110**, 5568 (1999).

³⁸W. Müller and W. Meyer, *J. Chem. Phys.* **85**, 953 (1986).

³⁹S. Ivanov, S. Hirata, and R. J. Bartlett, *Phys. Rev. Lett.* **83**, 5455 (1999).

⁴⁰A. Görling, *Phys. Rev. Lett.* **83**, 5459 (1999).